Non-Destructive Testing in the Automotive Supply Industry
- Requirements, Trends and Examples Using X-ray CT

Ralf B. Bergmann, Florian T. Bessler and Walter Bauer
Robert Bosch GmbH, Corporate Sector Research and Advance Engineering, Department of Applied Physics (CR/ARP), Robert-Bosch-Platz 1, 70839 Gerlingen-Schillerhöhe, Germany, Ralf.Bergmann@de.bosch.com

Abstract: Requirements on components for automotive applications are becoming evermore stringent. Defects need to be banned and dimensional measurement of complex geometries with high resolution is required. In addition, throughput is high and production cycles may last only a few seconds. These objectives call for non-destructive testing (NDT) that keeps step with the production cycle. Production and quality measurement techniques therefore play an important role in providing customers with more economical and reliable products. We briefly compare various NDT-techniques and demonstrate the feasibility of X-ray tomography as a technique suitable for the dimensional measurement of complex structures with sub-µm resolution.

1. Introduction: Why Do We Need Non-Destructive Testing (NDT)?

Demands on quality and reliability in the automotive and automotive supply industry are continuously rising. Zero defect quality is the goal, especially for components operating close to their physical load-limits or in safety relevant positions. Control of dimensional tolerances in some applications even requires sub-µm accuracy. Sometimes there is a need for in-line testing of all manufactured components (100%-testing). In-line testing also allows for process control and thus reduces waste production. In addition, NDT helps to speed up the development of new products and enables the rapid optimization of production processes.

2. Overview on NDT Techniques for Automotive Purposes

In this article, we distinguish two purposes of NDT: i) Detection of material defects and ii) dimensional measurements. Although there is a large variety of testing methods [1] only a few are really relevant for the testing of automotive components. While figures 1 compiles the main characteristics of these approaches for the detection of defects, figure 2 highlights the features of these methods for dimensional measurements.

Figure 1 shows the classification of X-ray computer-tomography (RCT or X-ray CT), ultrasonic (US) testing, eddy-current measurement and optical inspection techniques according to their penetration depth and their spatial resolution. Optical interferometry achieves by far the highest resolution. However, optical techniques can only monitor surfaces or coatings. In contrast, the best penetration depth (except for some highly absorbing materials such as Pb or Pt) combined with a high resolution is usually gained by X-

ray CT. In between these extremes, we find eddy current measurements for the detection of near-surface defects and US-techniques with a high penetration depth but with a resolution limited to several 10 µm. Figure 2 shows the classification of the above mentioned techniques with respect to dimensional measurements. Here, the emphasis is on the measurement of geometrical parameters, e.g. the geometry of components as compared to construction (CAD) data. Again, the same trends as in Fig. 1 can be stated.

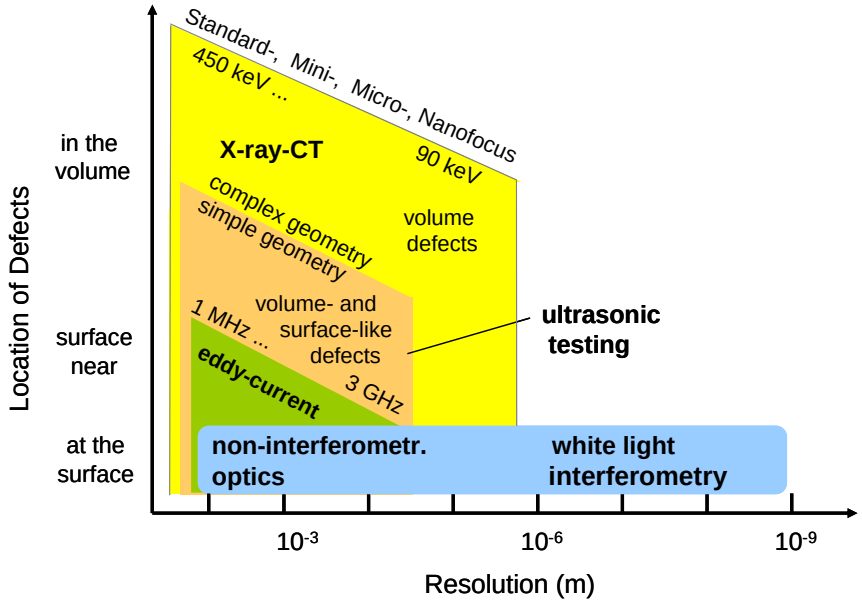

Figure 1: Classification and comparison of X-ray CT, ultrasonic testing, eddy current and optical measurement techniques (denoted as non-interferometrical optics and white light interferometry) according to detectable defect location and spatial resolution.

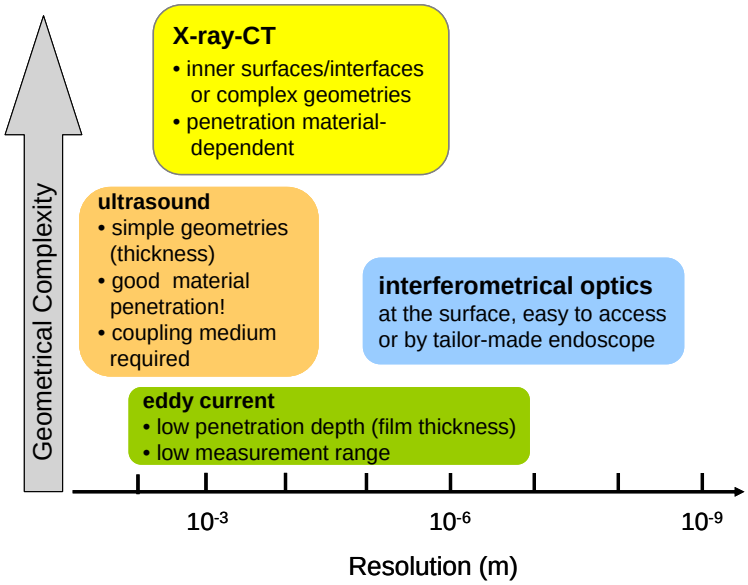

Figure 2: Classification of the non-destructive, geometrical measurement techniques discussed in fig. 1. according to geometrical complexity and resolution.

In this paper, we will focus on the analysis of hidden structures using X-ray CT [2]. A more extensive discussion and comparison with other techniques can be found in Ref. [1]. For the discussion of high-resolution optical measurement techniques see e.g. Ref. [3].

3. Principles, Limitations and Potential of X-Ray Computer Tomography (CT)

Figure 3 schematically outlines the essential components of a state of the art CT-system for industrial testing purposes. The main constituents are an X-ray source, a flat panel detector and the image acquisition and reconstruction hard- and software.

Apart from practical parameters, such as maximum material thickness to be penetrated by the X-rays and the maximum sample diameter limited by the size of the detector, the key parameters of such a setup are: i) the resolution (the minimum detectable feature size) and ii) the data collection and reconstruction time required for the analysis. According to our experience at Bosch, since the year 2000 resolution has improved by two orders of magnitude, while reconstruction time has improved by a factor of around 50. In the following subsections we will discuss the parameters essential for an improvement of both spatial resolution and reconstruction time.

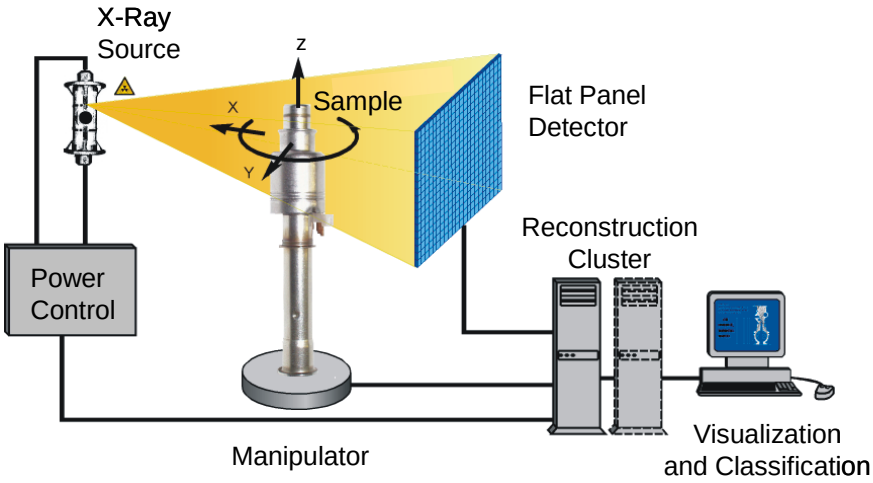

Figure 3: Set-up of an X-ray CT system for industrial testing purposes. The System consists of an X-ray source, a mechanical manipulator for rotating the sample, an X-ray flat panel detector and a (stack of) PCs for reconstruction and visualization.

3.1. Spatial resolution

The spatial resolution is primarily based on the voxel size V but should not be mis-interpreted as accuracy or resolution of the CT-system. As will be shown later, the accuracy of a dimensional measurement can be much better than V while for the case of defect detection V sets a lower limit to the detectable defect diameter.

The voxel size V of a CT-system depends on the geometrical magnification M, the pixel to pixel distance d_{det} of the detector and the target diameter d of the X-ray source. Figure 4a explains the geometry for the case of an infinitely small target ($d \rightarrow 0$). The magnification $M=FDD/FOD$ is given by the ratio of the focus to detector distance FDD and the focus to object distance FOD. In this ideal case, one obtains a low voxel size by choosing a very low value for FOD or a high value for FDD and thus a very large geometrical magnification M. The voxel size is then only determined by the pixel to pixel distance d_{det} of the detector and the magnification M resulting in $V = d_{det} / M$. For the practically relevant case of an X-ray source with a finite size, see fig. 4b, the target diameter d sets a lower limit to the useful voxel resolution. The width of the half shadow S is determined by d and the factor M limiting the minimum useful voxel size. As it does not

make sense to increase the magnification beyond the point where $S > d_{det}$, the maximum useful magnification (for $M >> 1$) is therefore limited to $M_{max} = d_{det} / d$.

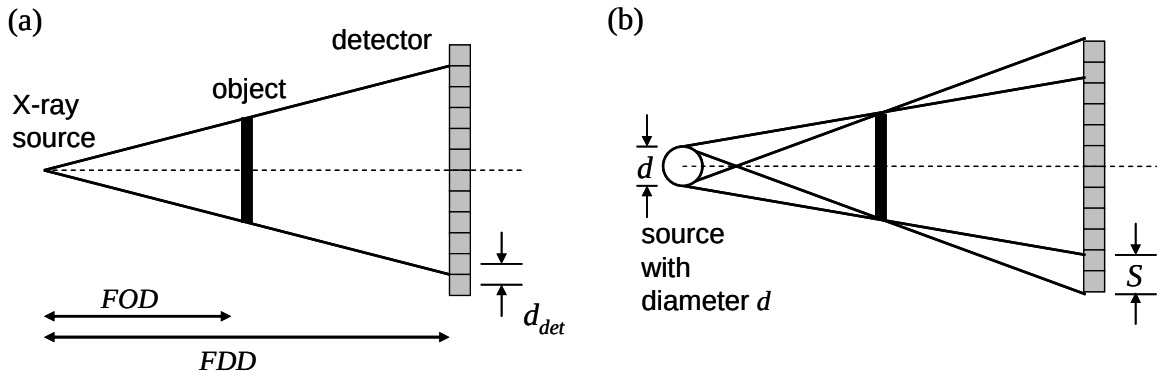

Figure 4: Geometric magnification of a CT setup, for an explanation of the symbols see text.

3.2. Reconstruction time

The data collection time for reconstruction depends on: i) The intensity of the X-ray source, ii) the quantum efficiency and iii) the data transfer rate of the detector. The total process time is, in addition, depending on the speed of the reconstruction. In the following discussion, the quality of X-ray sources will turn out to be one of the key factors for the advancement of measuring speed. Detectors have some room for improvement, but are not our primary focus. Concerning reconstruction speed, the development of computational power still follows Moore's law, therefore an increase of reconstruction speed appears predictable. In addition, improvements of algorithms will speed up reconstruction.

3.2.1. X-ray sources

In order to speed up the measurement process, one should employ an X-ray source with the highest possible intensity. However, the X-ray intensity is fundamentally limited by the maximum possible heat dissipation of the X-ray target. Exceeding a critical material dependent power density will result in evaporating the target. Therefore, higher intensity requires larger target area and therefore limits the resolution of the measurement. As a consequence, for obtaining high speed *and* high spatial resolution, one has to increase the brilliance of the X-ray tube which is defined as

$$B = \frac{P_{x-ray}}{A} \qquad \text{Eq.(1)}$$

with the power of the X-ray radiation $P_{x\text{-}ray}$ and the target area A. For constant target voltage U_{target} of the X-ray tube, $P_{x\text{-}ray}$ increases proportional to P_{el} which represents the electrical power $P_{el} = U_{target} \cdot I_{target}$ dissipated at the target with the target current I_{target}.

Figure 5 shows the historical development of power and brilliance of X-ray sources. In 1895, W. C. Röntgen discovered the existence of X-rays [4] by using an ion discharge tube, which is quite different from the X-ray tubes used today. We have only estimated the order of magnitude of the brilliance and power of this source since precise historical values are not available. A significant increase in power was gained by the development of a hot cathode electron tube in 1910. This principle for X-ray tubes is still in use today [5]. Further increase in power density was obtained by using a rotating anode, as heat dissipation is distributed to a much larger target area [6]. Developments in the second half

of the last century concentrated on downsizing the focus area by using mini-, micro- and sub-micron focus tubes. This kind of tubes use electrostatic or electromagnetic electron lenses to focus the electron beam onto the target, and they are now commercially available from several suppliers. Micro-focus tubes available today have a target voltage up to 250 kV. Due to electron scattering within the target, the focus diameter is limited to 15 µm. For voltages up to 50 kV, the focus diameters ranges down to just below 1 µm.

The limiting parameter for the brilliance is the heat dissipation at the target. As a consequence, the ratio of the electrical power and the focal diameter P_{el}/d has to be limited to a range of 1 … 2 W/µm. Latest not yet commercially available developments are the micro-focus rotating anode [7], that increases the brilliance up to an order of magnitude, although this technique can only be used with focus diameters down to 20 … 40 µm. A problem still arises during continuous operation at high power, since heat transport from the rotating anode within the vacuum is rather limited. Latest research results at Fraunhofer IZFP in Saarbrücken indicate that thin tungsten targets with a thickness of 1 … 2 µm on top of a diamond structure with superior thermal conductivity will improve the heat dissipation and allow for an increase in brilliance of a factor between 2 and 5 [8].

As can clearly be seen, both power and brilliance of X-ray sources have substantially increased due to the development of new anode principles. However, it is now necessary to make these concepts ready for long term operation and commercially available for CT systems.

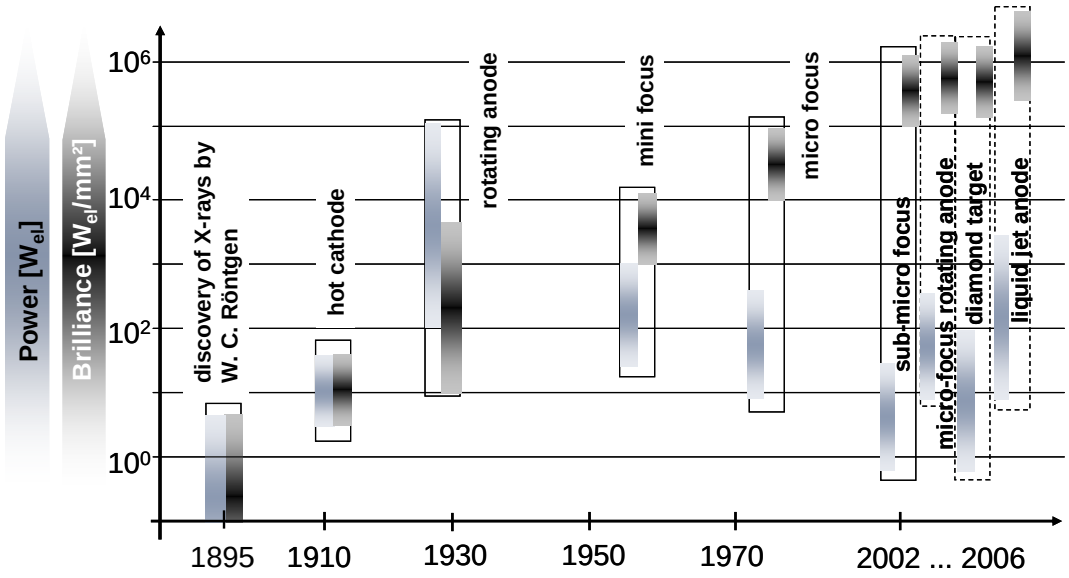

Figure 5: Development of X-ray tube performance: Following the discovery of X-rays in 1895, the brilliance developed by about six orders of magnitude due to the design of new X-ray sources. Latest developments represented within a dashed box are not jet commercially available. For reasons of comparability of literature data, the brilliance is here, in contrast to Eq.(1), based on the electrical power P_{el} per target area.

The main limitation for the solid targets employed in the X-ray sources described above is imposed by the heat dissipation required in order to compensate for the heat introduced by the electron beam. Due to the finite heat conductivity of a given solid, the temperature difference ΔT of the target as compared to the surroundings is determined by the law of thermal conductivity [9]

$$\Delta T = \frac{P_{el} L}{AK} \qquad \text{Eq.(2)}$$

with P_{el} = electron beam power dissipated at the target, L = length along which the heat is dissipated, A = area through which heat flows and K = heat conductivity of the target material.

For illustration we choose an X-ray source with an electron beam power of P_{el} = 10 W and a half-sphere shaped copper target, see fig. 6, that absorbs the electrical power of the electrons within a radius r_1 = 1 µm and an area $A = 2\pi r_1^2$. The temperature difference ΔT follows from an integration between r_1 and r_2. Choosing r_2 = 2 µm or r_2 = 10 µm and using the excellent heat conductivity of copper of K = 400 W/(m·K), we calculate a temperature difference

$$\Delta T = \frac{P_{el}}{2\pi K}\int_{r_1}^{r_2}\frac{dr}{r^2} = \frac{P_{el}}{2\pi K}\left(\frac{1}{r_1}-\frac{1}{r_2}\right). \qquad \text{Eq. (3)}$$

This calculation assumes (as a good approximation) that the electrons uniformly heat the target half sphere within the radius r_1 = 1µm. With the parameters given above, we obtain ΔT = 1990°K for r_2 = 2 µm and ΔT = 3580°K at r_2 = 10 µm. As a consequence, copper will melt or evaporate under these conditions because of its boiling point at 2595°K. The same is true for tungsten, since it has a much lower heat conductivity of 174 W/(m·K) as compared to copper, which would increases ΔT up to 8232°K (boiling point 5930°K).

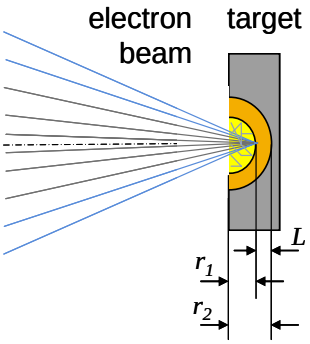

Figure 6: Simplified model of heat dissipation in a target.

As a consequence of these considerations, Hertz and coworkers have designed a liquid metal jet anode [10], that uses a liquid metal jet as an anode in order to overcome the limitations described above. The approach is expected to boost the power and brilliance of X-ray sources by about two orders of magnitude as compared to today's compact X-ray tube sources.

3.2.2. X-ray detectors

Important parameters of X-ray detectors are i) quantum efficiency, ii) number of pixels, iii) read out speed (frame rate) and iv) dynamic range. X-ray detectors have a quantum efficiency of about 2 … 50 % which strongly depends on the energy of the radiation and decreases with increasing energy. Improvements are expected in terms of data throughput, durability and dynamic range. An important milestone in the development of detectors is the flat panel detector which guarantees geometrical precision of the pictures and efficient transport of the light from the scintillator to the photodiodes. Another milestone is the utilization of directly converting detection principles (e.g. CdTe flat panel detectors [11]). These are available with high efficiency and high frame rate but less quality in some other features e. g. dynamic range and hot or dead pixels and have smaller number of pixels and possible segment displacement. The improvement of flat panel detectors using scintillation

technology was primarily based on increasing the number of pixels (up to the range of 10^7 pixels) and the size of the detector. The maximum dynamic range of flat panel detectors is 16 bit and is not expected to increase. The frame rate of large area detectors is in the range of 2 … 9 fps and is also not expected to grow substantially.

3.2.3. Hard- and software for reconstruction

In spite of several approaches such as e.g. correction of beam hardening [12], region of interest reconstruction and reconstruction from projections of incomplete angles, in practice almost always the standard Feldkamp back projection algorithm [13, 14] is used for reconstruction of volumetric data.

Continuous advances in computational power lead to the conclusion that reconstruction time is no longer the limiting parameter for the speed of CT. The image acquisition time now appears to be the critical parameter in order to find an optimum compromise between measurement time and image quality.

4. Examples of NDT of Automotive Components

4.1. Dimensional measurement of fuel injection channels with sub-voxel resolution

In order to optimize the configuration of a CT-system in view of the needs for NDT of automotive parts, we have built a CT-system from components rather than buying a complete system. Our in-house developed CT-system employs a 225 kV micro focus X-ray source and various X-ray detectors. The whole configuration is shielded by a lead cabin to ensure radiation safety. Details of components, setup and data evaluation are presented elsewhere [15]. Current research [16, 17] indicates the suitability of CT for dimensional measurement purposes in production measurement technology.

As mentioned above, the resolution of an X-ray system for defect detection is limited by the voxel size (choosing a reasonable geometric magnification). In a practical situation, a defect has to extend over at least two voxels to be identified. For dimensional measurements, however, subvoxel interpolation can be employed to significantly enhance the resolution. If, in addition, a-priori knowledge is available, e.g. geometries of a known type are to be evaluated, voxel statistics can help to further increase the resolution. As an example, figure 7 shows a reconstruction of the six injection channels of a fuel injector. For details of the evaluation and reconstruction see Ref.[15].

Subvoxel interpolation: In principle, the grey value of a voxel that belongs to the transition between air and material in the 3D data set represents the percentage of this voxel belonging to material rather than belonging to air. An approach that accounts for this interpretation of grey values is known as sub-voxel interpolation. If the interpretation of data is not obscured by noise, one can extract the position of a wall or interface much more precisely as compared to the size of the corresponding voxels. In the presence of noise, the uncertainty of the determination of the position of the wall ΔD depends on the Signal to Noise Ratio (SNR) of the data and the length of the voxels V according to

$$\Delta D = \frac{V}{SNR} \qquad \text{Eq.(4)}$$

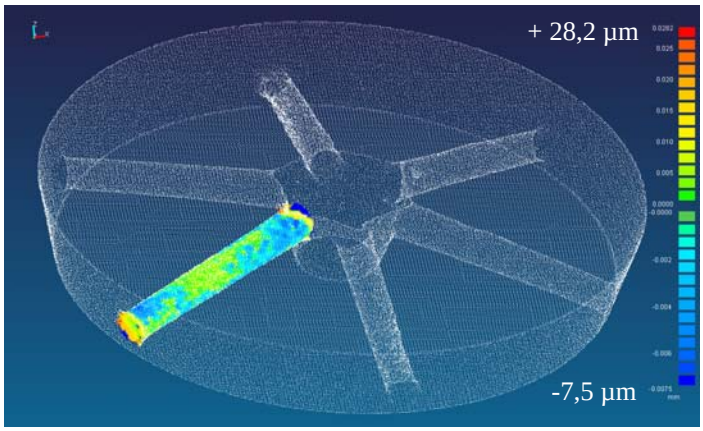

Figure 7: Reconstruction of the six injection channels of a fuel injector. The colors in the lower left channel show the deviation from a conical profile.

Voxel statistics: Using the grey values of all n voxels, that form the surface of a known geometry, e.g. an injection channel with the diameter D, it should be possible, to reduce the measurement error ΔD of the measurement of the channel diameter by a factor of

$$\Delta D = \frac{V}{SNR\sqrt{n}}. \qquad \text{Eq.(5)}$$

For the measurement of an injection channel with a diameter of around 150 µm and a length of 0.8 mm corresponding to around 5000 voxels each having a size of 7 µm and a SNR = 5 we therefore expect ΔD = 0.02 µm. The SNR could be significantly enhanced by increasing the measurement time. We have, however, obtained the complete CT in 8 min in order to approach realistic inspection times in production. In order to determine the accuracy of our CT system in combination with the use of sub-voxel interpolation, we have performed repeated measurements of the same injection channel several times.

Figure 8 shows the distribution of channel diameters over the 25 individual measurements. In order to minimize the influence of instabilities arising from the mechanical setup by changing the sample we have not detached the sample from the manipulator between the individual measurements. Assuming a Gaussian distribution, we obtain an average diameter of 146.8 µm and a standard deviation of σ = 0.15 µm from this set of measurements. This standard deviation, however, refers only to the relative precision of the measurement. In order to determine the absolute precision, one has to calibrate the CT measurement against a "golden part" with precisely known dimensions.

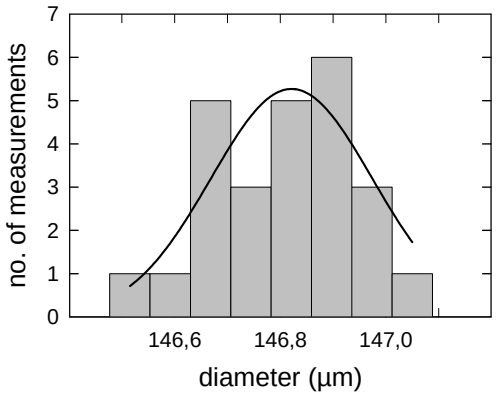

Figure 8: Histogram of 25 measurements of the diameter of an injection channel.

The difference between the experimental result and the expectation expressed in Eq.(5) may arise from influences such as the stability of the source and mechanical or thermal drift within the setup. Other measurements on nozzles, including a change of samples, show a standard deviation of $\sigma = 0.4$ µm. With these measurements, we have clearly demonstrated the achievement of sub-voxel resolution under realistic measurement conditions. Deviations from the theoretically expected accuracy have to be further clarified.

4.2. Portable Mini-CT system

In addition to the laboratory system described above, we have set up a mobile CT system. This so called "Mini-CT" demonstrates the feasibility of CT for mobile applications e.g. for defect detection and is the first step for an integration in a production line. Figure 9a shows a picture of the system shielded with a 20 mm thick steel housing. The housing has a volume of only $55 \times 18 \times 20$ cm³. Apart from the rotational axis none of the axes of the manipulator are motorized in order to minimize manipulator introduced measurement errors. The Mini CT consists of a Kevex X-ray source with an acceleration voltage of 90 keV, a beam current of 90 µA and a focus diameter of 5 … 8 µm and an Hamamatsu detector with 1032×1032 pixels with a pixel to pixel distance of 50 µm and 12 bit resolution of the AD-converter.

(a)

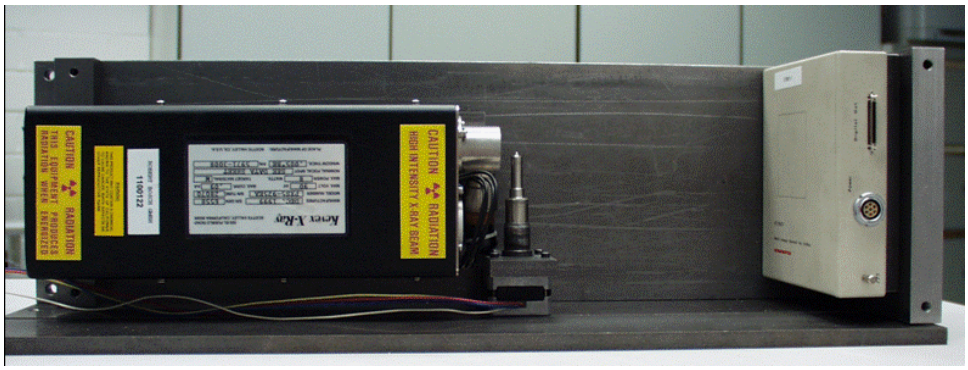

(b)

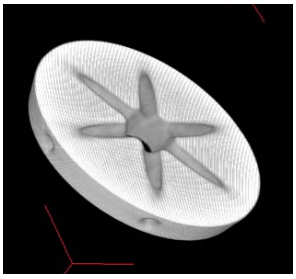

(c)

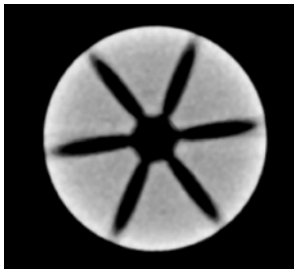

Figure 9: a) Mini-CT System with part of the housing removed for visibility of the components. Left: X-ray source, center: manipulator with sample (fuel injector), right: detector. Footprint 55×18 cm^2, b) 3D picture and c) projection of a slice of an injector obtained from CT. Diameter of the cross section is approx. 2 mm.

Figure 9b and c show different views of the reconstruction of the nozzles of a Diesel injector collected with the Mini-CT. These data are comparable to the data used for the calculation of the values of Figure 8. The data are collected with the same detector and a comparable rotation system only using another X-ray tube with 120 kV acceleration voltage. Due to a longer measurement time the SNR of the dataset is not visibly different. We therefore estimate that the Mini-CT system should have an accuracy comparable to the laboratory setup discussed in paragraph 4.1.

5. Summary, Future Trends and Requirements

We have outlined the importance of non-destructive testing (NDT) for defect detection and dimensional measurements of automotive components. Several NDT techniques are in use in the automotive supply industry to achieve zero defect quality. For the observation of hidden or complex geometries or defects in such components, X-ray tomography appears to be well suited as a measurement tool. However, cost, speed and accuracy of X-ray CT have up to now impeded it's widespread use. We have shown, using fuel injectors as an example, that comparatively fast CT measurements with sub-µm resolution are possible using commercially available CT-components and have demonstrated a mini-CT system aiming at in-line applications of X-ray CT.

Presently, the brilliance of X-ray sources appears to be the bottleneck for a significant increase in the speed of CT measurements. We conjecture that a significant increase in the application of CT-systems in the automotive industry is at hand, once X-ray sources with high brilliance and more cost effective custom designed and modular systems are commercially available.

References

[1] R.B. Bergmann, E. Zabler, Methoden der zerstörungsfreien Prüfung, in: *Handbuch der Mess- und Automatisierungstechnik in der Produktion*, 2nd Ed., Eds.: H.-J. Gevatter, U. Grünhaupt (Springer, Berlin, 2006), p. 363-410

[2] A. Kak, M. Slaney, Principles of Computerised Tomographic Imaging (IEEE Press, New York, 1988)

[3] R.B. Bergmann, P. Drabarek, U. Kallmann, B. Schmidtke, J. Bauer, Interferometrische Submikrometer-Messtechnik in der Automobilindustrie, Kap. 5.9-11 in: *Photonik – Grundlagen, Technologie und Anwendung*, Eds.: E. Hering, R. Martin (Springer, Berlin, 2006), p. 263 – 281.

[4] S. Flügge, Encyclopedia of Physics, Vol. XXX: X-Rays (Springer, Berlin, 1957), p. 1 ff

[5] see [4], p. 32

[6] see [4], p. 41

[7] A. Ramsay, G. Dermody, R. Hadland, I. Haig, The development of a high-precision microfocus X-ray computed tomography an digital radiography system for industrial applications, in: *Proc. BB84-CD, Int. Symposium on CT and Image Processing* (DGZFP, Germany, 2003), p. 61-69

[8] M. Maisl, Fraunhofer Institut für Zerstörungsfreie Prüfverfahren, Saarbücken, oral communication, 2005

[9] G.F.C. Rogers and Y.R. Mayhew, Engineering Thermodynamics (Longmans, London, 1962), p. 440

[10] M. Otendal, T. Tuohimaa, O. Hemberg, H. Herz, Status of the liquid-metal-jet-anode electron-impact x-ray source in X-Ray Sources and Optics, Eds.: C. Mac Donaled, A. Macrander, T. Ishikawa, C. Morawe, J. Wood, in: *Proc. of SPIE Vol.5537*, (SPIE, Bellingham, WA, 2004), p. 57-63.

[11] U. Ewert, U. Zscherpel, B. Redmer, C. Rädel, Neuer, direktwandelnder Festkörperdetektor auf der Basis von CdTe, in: *14th. Research group meeting "Industrielle Röntgenprüfverfahren"* (Fraunhofer Society, Fürth, Germany, 2003)

[12] Illerhaus B., Onel Y., Goebbels J., Correction techniques for 2D detectors to be used with high energy X-ray sources for CT, part II, in: *Developments in X-Ray Tomography IV, Proc. SPIE Vol. 5535*, Ed.: U. Bonse (SPIE, Bellingham, WA, 2004), p. 329-334.

[13] L. Feldkamp, J. Kress, L. Davis, J. Optical Society of America A **1**, 612-619 (1984)

[14] F. Natterer, The mathematics of computerised tomography, 1st Ed., (Wiley, New York, 1978)

[15] W. Bauer, F.T. Bessler, E. Zabler and R.B. Bergmann, Computer tomography for non destructive testing in the automotive industry, in: *Developments in X-Ray Tomography IV, Proc. SPIE Vol. 5535*, Ed.: U. Bonse. (SPIE, Bellingham, WA, 2004), p. 464-472.

[16] M. Bartscher, F. Wäldele, J. Göbbels, Genauigkeitssteigerung von industriellen Röntgen Computer-tomographie (CT)- Anlagen für die dimensionelle Messtechnik, in: *Proc. of DGZFP Jahrestagung in Salzburg* (DGZFP, Berlin, 2004), P 17

[17] D. Imkamp, H. Lettenbauer, B. Georgi, Computertomographie für die dimensionelle Fertigungs-messtechnik – Status und Potentiale, in: *Sensoren und Messsysteme, 13. ITG/GMA Fachtagung* (VDE-Verlag, Berlin, 2006), p. 117-120.